Effects of Ca2+ on supramolecular aggregation of natural organic matter in aqueous solutions: A comparison of molecular modeling approaches

Andrey G. Kalinichev, E. Iskrenova-Tchoukova, W.-Y. Ahn, M. Clark, J. Kirkpatrick

Submitted to *Geoderma*: June 24, 2010. Accepted, updated September 7, 2010.

Effects of Ca^{2+} on Supramolecular Aggregation of Natural Organic Matter in Aqueous Solutions: A Comparison of Molecular Modeling Approaches

Andrey G. Kalinichev,[a,b,*] Eugenia Iskrenova-Tchoukova,[a] Won-Young Ahn,[c,1]

Mark M. Clark,[c,2] R. James Kirkpatrick[d]

[a] Department of Chemistry, Michigan State University, East Lansing, MI 48824, USA,

[b] Department of Geological Sciences, Michigan State University, East Lansing, MI 48824, USA

[c] Department of Civil and Environmental Engineering,

University of Illinois at Urbana-Champaign, Urbana, IL 61801, USA

[d] College of Natural Science, Michigan State University, East Lansing, MI 48824, USA

[1] *Present address:* Water Business Group, Doosan Heavy Industries & Construction Co., Ltd,

South Korea

[2] *Present address:* Department of Civil and Environmental Engineering,

Northwestern University, Evanston, IL 60208, USA

[*] Corresponding author:
Present address: Laboratoire SUBATECH, Ecole des Mines de Nantes, 4 rue Alfred Kastler, La Chantrerie – BP 20722, 44307 Nantes Cedex 3, FRANCE

E-mail: kalinich@subatech.in2p3.fr
Tél: +33 2.51.85.84.80 / Fax : +33 2.51.85.84.79

Abstract

Natural organic matter (NOM) represents a complex molecular system that cannot be fully characterized compositionally or structurally in full atomistic detail. This makes the application of molecular modeling approaches very difficult and significantly hinders quantitative investigation of NOM properties and behavior by these otherwise very efficient computational techniques. Here we report and analyze three molecular dynamics (MD) simulations of Ca^{2+} complexation with NOM in aqueous solutions in an attempt to quantitatively assess possible effects of model- and system size-dependence in such simulations. Despite some obvious variations in the computed results that depend on the size of the simulated system and on the parameters of the force field models used, all three simulations are quite robust and consistent. They show Ca^{2+} ions associated with 35-50% of the NOM carboxylic groups at near-neutral pH and point to a strong preference for the stability of bidentate-coordinated contact ion pairs. The degree and potential mechanisms of NOM supramolecular aggregation in the presence of Ca^{2+} ions in solution are also assessed on a semi-quantitative level from two larger-scale MD simulations.

1. Introduction

Natural organic matter (NOM) is ubiquitous in the environment and plays many important geochemical roles by forming aqueous complexes of widely differing chemical and biological stabilities with inorganic and organic species (Buffle, 1988; Sposito, 1989; Stevenson, 1994; Tipping, 2002). Metal-NOM interactions induce strong correlations between the concentration of natural organic matter and the speciation, solubility and toxicity of many metals in the environment. In the technological processes of water purification and desalination, NOM is implicated as the major foulant of ultrafiltration, nanofiltration and reverse osmosis membranes (Jucker and Clark, 1994; Hong and Elimelech, 1997; Howe and Clark, 2002; Li and Elimelech, 2004; Lee and Elimelech, 2006; Ahn et al., 2008), either directly or by forming a surface conditioning layer for microbial attachment ("biofouling"). Despite significant geochemical, environmental and technological interest, the molecular-level mechanisms and dynamics of the physical and chemical processes involving NOM are not yet well understood.

Computational molecular modeling has long been recognized as a very powerful tool to study such phenomena in true atomistic detail at the nanoscale in both space and time (e.g., Schulten and Schnitzer, 1993,1997; Kubicki and Apitz, 1999). However, for NOM this route presents significant challenges due to the extraordinary molecular diversity of NOM, which precludes its unique atomistic description. NOM is a complex mixture of many components with varying composition and structure depending on the sample origin, extraction procedure and other experimental conditions (Piccolo, 2002; Leenheer and Croué, 2003; Wershaw, 2004; Sutton and Sposito, 2005; Leenheer, 2009). On the other hand, the principal functional groups of NOM are quite well characterized and understood (e.g., Stevenson, 1994; Piccolo, 2002; Simpson et al., 2002; Leenheer and Croué, 2003; Wershaw, 2004; Sutton and Sposito,2005), and

the proposed NOM models have many common features.

There have been several efforts to develop molecular models of NOM. Schulten and Schnitzer used analytical pyrolysis measurements to develop a series of NOM structural models (Schulten and Schnitzer, 1993, 1997; Schulten, 1999). One of these models was recently used in MD simulations of NOM interaction with hydrated Na^+ and Ca^{2+} ions (Sutton et al., 2005). Shevchenko and Bailey (1998a,b) have simulated NOM sorption on soil mineral particles using an NOM model based on an oxidized lignin-carbohydrate complex. Leenheer et al. (1998) have proposed a molecular model of Suwannee River fulvic acid and used it for the interpretation of experimental data on metal-NOM binding. Kubicki and Apitz (1999) used this model to compare the structures computed by classical molecular mechanics and quantum (semi-empirical and Hartree-Fock) calculations and to test the effect of computational methodology on the predicted structure. This model was also later used in the molecular simulation of hydrogen bonding and clustering of neutral fulvic acid fragments in aqueous solution (Porquet et al., 2003). Diallo et al. (2003) applied an algorithm of computer-assisted structure elucidation (CASE) to a comprehensive set of spectroscopic and analytical data for Chelsea soil humic acid and developed a series of representative 3-D structural models for these substances. The Temple-Northeastern-Birmingham (TNB) model of an NOM building block was derived by Davies et al. (1997) and then successfully used in a conformational modeling study (Sein et al., 1999). We have also recently used this model for the molecular simulations of metal-NOM complexation in bulk aqueous solutions (Xu et a., 2006; Kalinichev and Kirkpatrick, 2007; Iskrenova-Tchoukova et al., submitted) and for the computer simulations of the effects of metal ions on the NOM adsorption at the surfaces of polyethersulfone ultrafiltration membranes (Ahn et al., 2008)

Thus, notwithstanding all the differences and uncertainties in the detailed atomistic

characterization of NOM, computational molecular modeling of NOM-containing systems and processes can be very useful and instructive. Here we present a comparison of three molecular MD simulations using three different force field parameterizations for the same TNB model of NOM. Our results clearly indicate that despite the significant uncertainties inherent to the computational modeling of NOM, the simulation show only a moderate model dependence and are all quite robust in terms of their qualitative and even quantitative reproduction of the most significant structural, dynamic, end energetic characteristics of metal-NOM complexation, hydration, and supramolecular aggregation. The results of MD simulations also point out the need for computer simulations at much larger time and length scales and with more complex and diverse NOM models in order to fully quantify the phenomena of supramolecular aggregation of NOM in aqueous environments.

2. Molecular Dynamics Simulations of Ca-NOM Systems

The TNB model of an NOM molecular fragment used in all three simulations discussed below has a molecular weight of 753 Da and contains three carboxylic groups, three carbonyl groups, two phenolic groups, two amine groups, and four other R-OH alcohol groups (Jansen et al., 1996; Davies et al., 1997; Sein et al., 1999). The size, composition and molecular structure of the TNB model of NOM fragment is illustrated in Figure 1. In terms of the molecular weight, atomic composition, degree of aromaticity and total charge density the TNB model fragment is in good agreement with available experimental characterizations of NOM (Piccolo, 2002; Simpson et al., 2002; Leenheer and Croué, 2003), the results of stochastic modeling approaches based on computer assisted 3-D structure elucidation (Diallo et al., 2003), and biogeochemical reconstructions (Cabaniss et al., 2007). The composition of the TNB model is also quite close to

the composition of Suwannee River NOM (SRNOM), which is often used in experiments as a typical representative of natural organic matter (e.g., Xu et al., 2006; Ahn et al., 2008). The compositions of several NOM models are compared with experimental data for SRNOM in Table 1.

For the neutral pH conditions modeled in our simulations, we assume the three carboxylic groups of the NOM fragments as completely deprotonated (pK_a values between 4 and 5), whereas the hydroxyl groups as always protonated (pK_a values of ~ 9). The deprotonated carboxylic groups of NOM are known to be the principal source of the NOM negative charge development at the near-neutral pH range (e.g., Hong and Elimelech, 1997; Ritchie and Perdue, 2003). These negatively charged carboxylic groups are the most important binding sites for metal cations (Tipping, 2002; Rey Castro et al., 2009), and Ca^{2+} appears to be among the most strongly NOM-associating ions (Leenheer et al., 1998; Wall and Choppin, 2003; Li and Elimelech, 2004; Brigante et al., 2007; Nebiosso and Piccolo, 2009).

Three separate MD simulations (Table 2) were performed for the same TNB model in aqueous solutions containing Ca^{2+} ions at approximately the same concentrations, but using different system sizes, different force fields, and two different water models in order to better understand is some quantitative detail the extent to which the results of such simulations can be expected to be model-specific. In the MD simulation Run I, a single TNB molecule was hydrated by 553 water molecules in a cubic box with standard periodic boundary conditions. The negative charge of the NOM fragment was balanced by the presence of two Ca^{2+} and one Cl^{-} ions in solution. The interatomic interactions among H_2O, dissolved ions and NOM were described by the SPC water model (Berendsen et al., 1981), SPC-compatible parameters for the ions (Åquist, 1990), and the consistent valency force field (CVFF) for the NOM (Kitson and Hagler, 1988).

For the MD Runs II and III, the simulation cells were almost an order of magnitude larger and contained 8 TNB fragments and 12 Ca^{2+} cations hydrated by more than 4000 H_2O molecules (Table 2). In the Run II, the CHARMM27 force field (MacKerell et al., 1998) was employed to describe all interatomic interactions in the system, whereas in the Run III the AMBER FF99 force field (Case et a., 2006) was employed. In both of these simulations water was described by the TIP3P molecular model (Jorgensen et al., 1983).

In all three simulations, a time step of 1 fs was used to numerically integrate the Newtonian equations of atomic motions, and Ewald summation (e.g., Allen and Tildesley, 1987) was applied to calculate long-range electrostatic contributions to the total intermolecular potential energy of the simulated systems. To assure proper thermodynamic equilibration and NOM conformational relaxation of the initial molecular models, the pre-equilibration MD runs were performed for each of the simulated system in several stages with the total simulation length of several hundreds of picoseconds. This pre-equilibration process resulted in simulated densities that corresponded well to an ambient pressure of 0.1 MPa. These optimized models were used as the starting configurations for the production MD simulations that were all performed in the *NVT* statistical ensemble at a constant temperature of 300 K and at constant volume.

The duration of production Run I was 100 ps, whereas the equilibrium Runs II and III were 100 times longer (10 ns each). These longer run times allowed us to determine not only the structural characteristics of Ca^{2+}-NOM complexation at individual binding sites, but also to quantitatively estimate the degree of supramolecular aggregation of NOM fragments in solution due to their strong electrostatic interactions with Ca^{2+} ions.

To quantitatively assess the structural and dynamic effects of Ca^{2+}-NOM complexation,

we calculated the radial distribution functions (RDFs) and running coordination numbers using standard procedures (e.g., Allen and Tildesley, 1987). The running coordination numbers of species *j* around species *i* in the solution, $n_{ij}(r)$, are calculated from the RDFs as

$$n_{ij}(r) = 4\pi\rho_j \int_0^r g_{ij}(r)\, r^2 dr\,, \tag{1}$$

where ρ_j is the number density of species *j* in the system, $g_{ij}(r)$ are the atom-atom RDFs.

Potentials of mean force (PMFs) for the interaction between the Ca^{2+} cations and the carboxylic groups of the NOM fragments were also calculated. The PMF characterizes the change in the free energy of the system due to the changes in its configuration (e.g., Kollman, 1993). If the free energy of a system in thermodynamic equilibrium in the *NVT* statistical ensemble is

$$F = -k_B T \ln Z\,, \tag{2}$$

where *Z* is the canonical partition function and k_B is the Boltzmann constant, then the potential of mean force, $W(r)$, for two interacting species is defined as the potential that would generate the mean force between the two species, averaged over all orientations, for each separation distance *r*. Thus, the PMF represents the free energy profile of the system as a function of *r*, and it can be shown (e.g., McQuarrie, 2000) that

$$W(r) = -k_B T \ln g(r), \tag{3}$$

where $g(r)$ is the corresponding radial distribution function for this pair of species with the standard normalization for large separations, $g(r) \rightarrow 1$ at $r \rightarrow \infty$. Thus, $W(r)$ asymptotically approaches zero with large separation distance. The PMF calculations for the metal cation complexation with the carboxylic groups of NOM molecules and the resulting estimates for the metal-NOM association constants are discussed in detail elsewhere (Iskrenova-Tchoukova et al.,

submitted).

3. Results and Discussion

There are three structurally distinct carboxylic groups in the TNB molecular model of NOM used in our simulations (Figure 1). Ca^{2+} cations can associate with these carboxylic groups via several typical and relatively stable coordination geometries (Iskrenova-Tchoukova et al., 2010). In a *bidentate* inner-sphere coordination (at the bottom of Figure 1), Ca^{2+} is coordinated simultaneously with the two oxygen atoms of the carboxylic group and stays approximately equidistant from both of them predominately near the bisector plane orthogonal to the plane of the carboxylic group. In a *monodentate* inner-sphere coordination (at the top of Figure 1), the Ca^{2+} ion is coordinated with only one of the carboxylate oxygen atoms. Thus, in both bidentate and monodentate cases, the water molecules in the first coordination shell of Ca^{2+} are partially replaced by the carboxylate oxygens. In contrast, in an outer-sphere coordination, the Ca^{2+} ion is separated from the NOM carboxylate oxygens by a mono-molecular layer of H_2O, and one can consider this coordination as a fully hydrated Ca^{2+} ion weakly associated with the carboxylic group forming a solvent separated ion pair.

The radial distribution functions of for Ca^{2+} ions coordinating carbon atoms of the NOM carboxylic groups for all three simulations are shown in Figure 2 (thick lines, left scale) together with the running coordination numbers (thin dashed lines, right scale). For the small system size of Run I, one out of two Ca^{2+} ions was associated with one of the three available carboxylic groups and stayed in an inner-sphere bidentate coordination for almost the entire length of the simulation (Kalinichev and Kirkpatrick, 2007). This resulted is the single sharp RDF peak around 2.8 Å and a statistical estimate of about 35% carboxylic groups being coordinated by

Ca^{2+} ions in such solutions. Remarkably, this result holds quite well even in much longer simulations, for much larger systems, and for the different force field parameterizations of Runs II and III. The results of Run III show about the same fraction of the Ca-occupied carboxylic groups in the inner-sphere coordination as Run I, whereas Run II indicates a somewhat higher degree of association, of the order of 50%.

However, the simulations for these larger systems reveal the structure of the first and second coordination spheres of the NOM carboxylic groups in significantly more detail then before (Kalinichev and Kirkpatrick, 2007). In particular, it is evident that the bidentate coordination of Ca^{2+} is significantly more pronounced than the monodentate coordination among the contact ion pairs (CIP) in the simulation of Run II, compared of a similar Run III. This is clearly a model-dependent effect due to a somewhat smaller size of the Ca^{2+} ion assumed in the CHARMM force field, which allows the cations to more closely approach the negatively charged NOM functional groups, thus resulting in stronger binding (thick red line in Figure 2). This effect could also be partially responsible for the higher degree of the Ca-NOM association observed in this simulation. However, both Run II and Run III are quite consistent in probing the outer-sphere coordination environment of the carboxylic groups in Ca-NOM aqueous solutions at distances from 4 to 6.5 Å. In both cases, they indicate that about 15-20% of the carboxylic groups are additionally found in this coordination, which can also be interpreted as solvent-separated ion pairing (SSIP).

These results are in good agreement with available experimental observations of Ca-NOM complexation (Leenheer et al., 1998; Wall and Choppin, 2003; Li and Elimelech, 2004; Brigante et al., 2007; Nebiosso and Piccolo, 2009) and also qualitatively consistent with another MD simulation for a similar system (Sutton et al., 2005). However, a direct quantitative

comparison with this latter molecular modeling work is not possible because of the different settings in which the simulations were performed. All three of our MD simulations employed the relatively small TNB model fragment, but used periodic boundary conditions with a large number of H_2O molecules. This allowed us to create a realistic model of NOM hydration and ionic complexation in bulk aqueous solution with unrestricted ion exchange among inner-sphere, outer-sphere, and bulk-solution environments. On the other hand, Sutton et al. (2005), while employing a much larger (10,419 Da) and more complex NOM model (Schulten, 1999) but ran their MD simulation without periodic boundary conditions. Their NOM molecule was only hydrated by a thin, approximately 5.0 Å, layer of water, and all the cations were originally placed within 5.2 Å of the NOM carboxylic groups. Both of these circumstances can lead to a bias in favor of the ions occurring in CIP and SSIP coordinations and the thin water shell completely precludes the possibility of the ions occurring in a fully hydrated, bulk-solution environment. Nonetheless, the qualitative similarity among our three simulations and that of Sutton et al. (2005) is another encouraging fact clearly suggesting that the fundamental character of the Ca-NOM interactions is not highly model-dependent and can be reliably captured in classical MD simulations.

The detailed analysis of Ca^{2+} dynamics around the NOM carboxylic groups conducted for Run III shows that an average residence time of a bidentate coordinated CIP is about 0.5 ns, compared with the about 0.1 ps for a monodentate CIP coordination, and about 0.2 ns for a SSIP coordination (Iskrenova-Tchoukova et al., 2010). These values provide useful estimates for the time scale for the processes of Ca-NOM association in aqueous solutions and point out to the fact that our earlier simulation (Kalinichev and Kirkpatrick, 2007), presented here as Run I, was not long enough for reliable quantitative estimates of the structure and dynamics in this system

(Table 2).

A comparison of potentials of mean force calculated for Runs II and III according to Eq.3 for Ca^{2+} interaction with the carboxylic groups of NOM is presented in Figure 3. Both simulations consistently result in a potential well –3.0±0.5 kcal/mol deep for bidentate CIP coordination with an interatomic separation of about 3.0 Å and in a shallower and broader potential well of –0.7±0.2 kcal/mol at about 5.5 Å corresponding to a SSIP coordination. However, the potential barrier between the CIP and SSIP coordinations is higher by almost 1 kcal/mol for Run II than for Run III, indicating a stronger preference for inner-sphere vs. outer-sphere coordination for the latter model. Consistent with the structural results discussed above, such model dependence is even more visible in the energy of monodentate-coordinated CIPs between Runs II and III. For the former, the corresponding potential well (red line in Figure 3 at about 3.5 Å) is located in the region of positive energies, indicating that such coordinations, although relatively stable, are generally unfavorable.

Another aspect of a model dependence of the simulated results is evident from the presence of distinct RDF peaks at 7.5 and 9.0 Å in Figure 2 (well reproduced in all three of our MD runs) and the corresponding PMF minima at the same distances in Figure 3. These features clearly appear at distances well beyond the typical range of strong site-site correlations and would seem to point to an unusually strong Ca-NOM association at unusually large intermolecular separations. However, careful analysis of the model structure helps to calrify the situation. Indeed, in the TNB model the carbon atoms of the two carboxylic groups (shown at the top and at the bottom of Figure 1) are located at two different ends of a nearly rigid aliphatic backbone. Thus, when a Ca^{2+} ion is associated with one of these carboxylic groups, the distance between the cation and the other carboxylic group also becomes nearly fixed creating an

impression of strong metal-carboxylate correlations at large distances. Thus, the two features in Figures 2 and 3 at 7.5 and 9.0 Å simply correspond to two different conformations of the aliphatic backbone of the TNB model, illustrating the model dependence of the MD simulated results for NOM-containing systems arising, in this case, not due to the variablility of the force fields used in the simulations, but due to the particular molecular structure of the modeled NOM fragment itself.

Ca^{2+} is known to play an important role in causing supramolecular aggregation of relatively small NOM fragments into larger colloidal particles (e.g., Leenheer et al., 1998; Wall and Choppin, 2003; Li and Elimelech, 2004; Baalousha et al., 2006; Brigante et al., 2007; Nebiosso and Piccolo, 2009). We have attempted to quantify this process in the Run II simulation by monitoring the RDFs for centers of mass (COM) of the TNB fragments as a function of time. The entire 10 ns MD-simulated trajectory was divided into 10 blocks, 1 ns each, and the COM-COM radial distribution functions were calculated separately for each block, along with the corresponding running coordination numbers (Eq. 1). These curves are presented in Figure 4 for the first and the last nanosecond of the trajectory. The increase of the molecular density at intermolecular distances of 12-15 Å is a clear indication of the ongoing aggregation process. At the beginning of the simulation, virtually none of the TNB fragments had any nearest neighbors at distances as close as 15 Å, wheras each of them had on average one such neighbor after about 10 ns of the dynamical evolution.

Qualitatively similar results were obtained from the analysis of Run III (Iskrenova-Tchoukova et al., submitted). A snapshot from this latter simulation is presented in Figure 5, where three aggregating TNB fragments are shown in different colors, Ca^{2+} ions are shown as the light blue balls, and all H_2O molecules are removed for clarity. One Ca^{2+} ion is found in a

strong inner-sphere bidentate coordination with the carboxylic groups of two NOM molecules (red and dark blue in Figure 5) and, simultaneously, in a weaker monodentate or outer-sphere coordination to a third NOM molecule (yellow in Figure 5).

A simultaneous coordination of Ca^{2+} ion by two carboxylic groups of the same NOM molecule was also observed in Run III in clear confirmation of an earlier hypothetical picture of Ca^{2+} capable to accept up to four NOM carboxylic groups in its inner-sphere coordination shell (Leenheer et al., 1998). This observation also suggests that the NOM complexation with Ca^{2+} may affect the supramolecular aggregation in two different ways. Ca^{2+} ions can directly affect aggregation by bridging carboxylic groups of different NOM molecules, effectively bringing and holding them together. In addition, simultaneous Ca^{2+} coordination with two carboxylic groups of the same NOM molecule, as observed in Run III, produces a metal-NOM complex with reduced net negative charge, thus allowing such complexes to approach each other more readily and, thus, to coordinate with each other via weaker hydrogen bonding interactions. Comparison of the simulations discussed here makes it clear that the size and the duration of the MD simulations should be increased at least another order of magnitude before statistically meaningful quantitative estimates for the relative importance of the two aggregation mechanisms could be to provided.

4. Conclusions

NOM is a good example of a complex material which, for natural reasons, cannot be fully characterized in full atomistic compositional and structural detail. This makes it particularly hard to approach a quantitative investigation of NOM behavior with traditional molecular modeling techniques. Here we have analyzed and quantitatively assessed the degree of possible model-

dependence in the results of such molecular computer simulations taking the complexation of Ca^{2+} with a realistic and well defined TNB model of NOM as an important example. The simulated results show some dependence on the size of the simulated system and on the parameters of the force field models used. We find it quite encouraging, however, that the main results are quite robust and are also consistent with available experimental data and other results of molecular modeling. All three of the simulations discussed here point to about 35-50% of the NOM carboxylic groups being associated with Ca^{2+} cations and provide extremely valuable information concerning the molecular structure, energetics, and dynamics of the association. This includes bidentate vs. monodentate configuration of the complexes, inner-sphere (CIP) vs. outer-sphere (SSIP) coordination of the ion pairs and their relative stability. The supramolecular aggregation of NOM in aqueous ionic solutions is also semi-quantitatively addressed in our simulations. However, much larger scale simulations (both in terms of the sizes of the modeled systems and the duration of the simulations) would have to be performed for Ca^{2+}–containing systems with different and more structurally diverse NOM models to further explore and quantify the phenomenon of aggregation, the relative importance of different aggregation mechanisms and the stability and dynamics of such aggregates.

Acknowledgments

This work was supported by the US Department of Energy, Office of Basic Energy Sciences, Division of Chemical Sciences, Geosciences, and Biosciences (grant number DE-FG02-08ER-15929) and by the NSF Science and Technology Center of Advanced Materials for Purification of Water with Systems (WaterCAMPWS) at the University of Illinois. The supercomputing resources of the NSF TeraGrid (grant number TG- EAR000002) and of the US

DOE National Energy Research Scientific Computing Center (NERSC) were used for the simulations.

References

Ahn, W. Y., Kalinichev, A. G., Clark, M. M., 2008. Effects of background cations on the fouling of polyethersulfone membranes by natural organic matter: Experimental and molecular modeling study. J. Membr. Sci. 309, 128-140.

Allen, M. P., Tildesley, D. J. 1987. Computer Simulation of Liquids. Oxford University Press, New York, 385 pp.

Åquist, J., 1990. Ion-water interaction potentials derived from free energy perturbation simulations. J. Phys. Chem. 94, 8021-8024.

Baalousha, M., Motelica-Heino, M., Coustumer, P. L., 2006. Conformation and size of humic substances: Effects of major cation concentration and type, pH, salinity, and residence time. Colloids and Surfaces A: Physicochem. Eng. Aspects 272, 48-55.

Berendsen H. J. C., Postma J. P. M., van Gunsteren W. F., Hermans J. 1981. Interaction models for water in relation to protein hydration. In: Intermolecular Forces (ed. B. Pullman), pp. 331-342. Riedel: Dordrecht, The Netherlands.

Brigante, M., Zanini, G., Avena, M., 2007. On the dissolution kinetics of humic acid particles: Effects of pH, temperature and Ca^{2+} concentration. Colloids and Surfaces A: Physicochem. Eng. Aspects 294, 64-70.

Buffle J., 1988. Complexation Reactions in Aquatic Systems: an Analytical Approach. Ellis Horwood Ltd, Chichester.

Cabaniss, S., Madey, G., Leff, L., Maurice, P., Wetzel, R., 2007. A stochastic model for the synthesis and degradation of natural organic matter part II: molecular property distributions. Biogeochemistry 86, 269-286.

Case, D. A., Darden, T. A., Cheatham, T. E., III, Simmerling, C. L., Wang, J., Duke, R. E., Luo,

R., Merz, K. M., Pearlman, D. A., Crowley, M., Walker, R. C., Zhang, W., Wang, B., Hayik, S., Roitberg, A., Seabra, G., Wong, K. F., Paesani, F., Wu, X., Brozell, S., Tsui, V., Gohlke, H., Yang, L., Tan, C., Mongan, J., Hornak, V., Cui, G., Beroza, P., Mathews, D. H., Schafmeister, C., Ross, W. S., Kollman, P. A. AMBER 9, University of California: San Francisco, 2006.

Davies, G., Fataftah, A., Cherkasskiy, A., Ghabbour, E. A., Radwan, A., Jansen, S. A., Kolla, S., Paciolla, M. D., Sein, L. T., Buermann, W., Balasubramanian, M., Budnick, J., Xing, B. S., 1997. Tight metal binding by humic acids and its role in biomineralization. J. Chem. Soc. Dalton Trans. 4047-4060.

Diallo, M. S., Simpson, A., Gassman, P., Faulon, J. L., Johnson, J. H., Goddard, W. A., Hatcher, P. G., 2003. 3-D structural modeling of humic acids through experimental characterization, computer assisted structure elucidation and atomistic simulations. 1. Chelsea soil humic acid. Environm. Sci. Technol. 37, 1783-1793.

Hong, S. K., Elimelech, M., 1997. Chemical and physical aspects of natural organic matter (NOM) fouling of nanofiltration membranes. J. Membr. Sci. 132, 159-181.

Howe, K. J., Clark., M. M. 2002. Fouling of microfiltration and ultrafiltration membranes by natural waters. Environ. Sci. Technol. 36, 3571-3576.

Iskrenova-Tchoukova, E., Kalinichev, A. G., Kirkpatrick, R. J., 2010. Metal cation complexation with natural organic matter in aqueous solutions: molecular dynamics simulations and potentials of mean force. Langmuir, accepted.

Jansen, S. A., Malaty, M., Nwabara, S., Johnson, E., Ghabbour, E., Davies, G., Varnum, J. M., 1996. Structural modeling in humic acids. Materials Science & Engineering C-Biomimetic Materials Sensors and Systems 4, 175-179.

Jorgensen, W. L., Chandrasekhar, J., Madura, J. D., Impey, R. W., Klein, M. L., 1983. Comparison of simple potential functions for simulating liquid water. J. Chem. Phys. 79, 926-935.

Jucker, C., Clark, M. M. 1994. Adsorption of aquatic humic substances on hydrophobic ultrafiltration membranes. J. Membr. Sci. 97, 37-52.

Kalinichev, A. G., Kirkpatrick, R. J., 2007. Molecular dynamics simulation of cationic complexation with natural organic matter. Eur. J. Soil Sci. 58, 909-917.

Kollman, P., 1993. Free energy calculations: Applications to chemical and biochemical phenomena. Chem. Rev. 93, 2395-2417.

Kubicki, J.D., Apitz, S.E., 1999. Models of natural organic matter and interactions with organic contaminants. Org. Geochem. 30, 911-927.

Lee, S., Elimelech, M., 2006. Relating organic fouling of reverse osmosis membranes to intermolecular adhesion forces. Environ. Sci. Technol. 40, 980-987.

Leenheer, J. A., 2009. Systematic approaches to comprehensive analyses of natural organic matter. Annals of Environmental Science 3, 1-130.

Leenheer, J.A., Brown, G.K., MacCarthy, P., Cabaniss, S.E., 1998. Models of metal binding structures in fulvic acid from the Suwannee River, Georgia. Environ. Sci. Technol. 32, 2410-2416.

Leenheer, J. A., Croué, J. P., 2003. Characterizing aquatic dissolved organic matter. Environ. Sci. Technol. 37, 18A-26A.

Li, Q., Elimelech, M., 2004. Organic fouling and chemical cleaning of nanofiltration membranes: measurements and mechanisms. Environ. Sci. Technol. 38, 4683-4693.

MacKerell, A. D., Bashford, D., Bellott, M., Dunbrack, R. L., Evanseck, J. D., Field, M. J.,

Fischer, S., Gao, J., Guo, H., Ha, S., Joseph-McCarthy, D., Kuchnir, L., Kuczera, K., Lau, F. T. K., Mattos, C., Michnick, S., Ngo, T., Nguyen, D. T., Prodhom, B., Reiher, W. E., Roux, B., Schlenkrich, M., Smith, J. C., Stote, R., Straub, J., Watanabe, M., Wiorkiewicz-Kuczera, J., Yin, D., Karplus, M. 1998. All-atom empirical potential for molecular modeling and dynamics studies of proteins. J. Phys. Chem. B 102, 3586-3616.

McQuarrie, D. A., 2000. Statistical Mechanics. 2 ed.; University Science Books: Sausalito, CA, 641 pp.

Nebbioso, A., Piccolo, A., 2009. Molecular rigidity and diffusivity of Al^{3+} and Ca^{2+} humates as revealed by NMR spectroscopy. Environ. Sci. Technol. 43, 2417-2424.

Piccolo, A., 2002. The supramolecular structure of humic substances: A novel understanding of humus chemistry and implications in soil science. Adv. Agronomy. 75, 57-134.

Pinheiro, J.P., Mota, A.M., Benedetti, M.F., 1999. Lead and calcium binding to fulvic acids: Salt effect and competition. Environ. Sci. Technol. 33, 3398-3404.

Rey-Castro, C., Mongin, S., Huidobro, C., David, C., Salvador, J., Garcés, J. L., Galceran, J., Mas, F., Puy, J., 2009. Effective affinity distribution for the binding of metal ions to a generic fulvic acid in natural waters. Environ. Sci. Technol. 43, 7184-7191.

Ritchie, J. D., Perdue E. M., 2003. Proton-binding study of standard and reference fulvic acids, humic acids, and natural organic matter. Geochimica et Cosmochimica Acta, 67, 85-96.

Schulten, H.R., Schnitzer, M., 1993. A state-of-the-art structural concept for humic substances. Naturwissenschaften 80, 29-30.

Schulten, H. R., Schnitzer, M. 1997. Chemical model structures for soil organic matter and soils. Soil Science 162, 115-130.

Schulten, H.R., 1999. Analytical pyrolysis and computational chemistry of aquatic humic

substances and dissolved organic matter. J. Anal. Appl. Pyrolysis 49, 385-415.

Sein, L. T., Varnum, J. M., Jansen, S. A., 1999. Conformational modeling of a new building block of humic acid: Approaches to the lowest energy conformer. Environ. Sci. Technol. 33, 546-552.

Shevchenko, S.M., Bailey, G.W., 1998a. Non-bonded organo-mineral interactions and sorption of organic compounds on soil surfaces - a model approach. Theochem J. Mol. Structure 422, 259-270.

Shevchenko, S.M., Bailey, G.W., 1998b. Modeling sorption of soil organic matter on mineral surfaces - Wood-derived polymers on mica. Supramolecular Science 5, 143-157.

Simpson, A., Kingery, W., Hayes, M., Spraul, M., Humpfer, E., Dvortsak, P., Kerssebaum, R., Godejohann, M., Hofmann, M., 2002. Molecular structures and associations of humic substances in the terrestrial environment. Naturwissenschaften 89, 84-88.

Sposito, G., 1989. The Chemistry of Soils. Oxford University Press, New York.

Stevenson, F. J., 1994. Humus Chemistry: Genesis, Composition, Reactions, 2nd ed. John Wiley, New York.

Sutton, R., Sposito, G., 2005. Molecular structure in soil humic substances: The new view. Environ. Sci. Technol. 39, 9009-9015.

Sutton, R., Sposito, G., Diallo, M. S., Schulten, H. R., 2005. Molecular simulation of a model of dissolved organic matter. Environ. Toxicol. Chem. 24, 1902-1911.

Tipping, E., 2002. Cation Binding by Humic Substances. Cambridge University Press, Cambridge, 434 pp.

Wall, N. A., Choppin, G. R., 2003. Humic acids coagulation: influence of divalent cations. Appl. Geochem. 18, 1573-1582.

Wershaw, R. L., 2004. Evaluation of conceptual models of natural organic matter (humus) from a consideration of the chemical and biochemical processes of humification. U.S. Geological Survey Scientific Investigations Report 2004-5121, U.S. Geological Survey, Reston, VA.

Xu, X., Kalinichev, A. G., Kirkpatrick, R. J., 2006. ^{133}Cs and ^{35}Cl NMR spectroscopy and molecular dynamics modeling of Cs^+ and Cl^- complexation with natural organic matter. Geochim. Cosmochim. Acta 70, 4319-4331.

Table 1 Composition of NOM building blocks according to several molecular models.

	C wt%	H wt%	O wt%	N wt%	S wt%	P wt%	carboxyl mol/kgC
TNB [a]	57.4	4.9	34.0	3.7	-	-	7.0
CSHA#9 [b]	53.3	4.2	37.9	1.4	3.0	-	9.3
Schulten [c]	51.5	4.0	41.8	2.0	0.6	-	14.3
Exp.(SRNOM) [d]	52.5	4.2	42.7	1.1	0.6	0.02	9.85

[a] Davies et al. (1997).

[b] Diallo et al. (2003).

[c] Sutton et al. (2005).

[d] Experimental data for Suwannee River NOM (Ritchie and Perdue, 2003) are given for comparison.

\

Table 2. Simulation parameters of the three Ca^{2+}-NOM aqueous solutions.

MD run	Force field	Simulation box size (Å)	Duration (ns)	Number of TNB	Number of Ca^{2+}	Number of Cl^-	Number of H_2O	Total number of atoms
I	CVFF[a]	25.55	0.1	1	2	1	553	1753
II	CHARMM27[b]	51.08	10	8	12	–	4191	13313
III	AMBER FF99[c]	51.32	10	8	12	–	4215	13385

[a] Kitson and Hagler (1988).

[b] MacKerell et al. (1998)

[c] Case et al. (2006)

FIGURE CAPTIONS

Figure 1. Molecular structure of the TNB model of the NOM fragment (Davies et al., 1997). The colors of the atoms are as follows: carbon – light gray , oxygen – red, hydrogen – white, and nitrogen – blue. The three carboxylic groups are shown in a ball and stick representation. Monodetate and bidentate and coordinated contact ion pairs are illustrated for the carboxylic groups at the top and the bottom of the figure, respectively.

Figure 2. Radial distribution functions (thick solid lines, left scale) and running coordination numbers (thin dashed lines, right scale) for carboxyl carbon – Ca^{2+} ion pairs from three different MD simulations discussed in the text.

Figure 3. Potentials of mean force for carboxyl carbon – Ca^{2+} ion pairs calculated for Runs II and III (red and blue lines, respectively).

Figure 4. Radial distribution functions (thick solid lines, left scale) and running coordination numbers (thin dashed lines, right scale) for the centers of mass of the TNB fragments calculated during the periods of 0-1 ns and 9-10 ns (red and black lines, respectively) from the equilibrium MD trajectory of Run II (red and blue lines, respectively).

Figure 5. A snapshot from the MD simulation of RunIII illustrating the NOM (TNB) aggregation in the presence of Ca^{2+} ions. H_2O molecules and other ions are removed for

clarity. Different TNB molecules are represented by different colors, whereas calcium ions are represented by blue spheres (not in scale). One Ca^{2+} is simultaneously coordinated by two carboxylic groups in bidentate configurations and by one carboxylic group in a monodentate configuration, whereas another Ca^{2+} is seen in a distorted bidentate inner-sphere coordination to yet another carboxylic group.

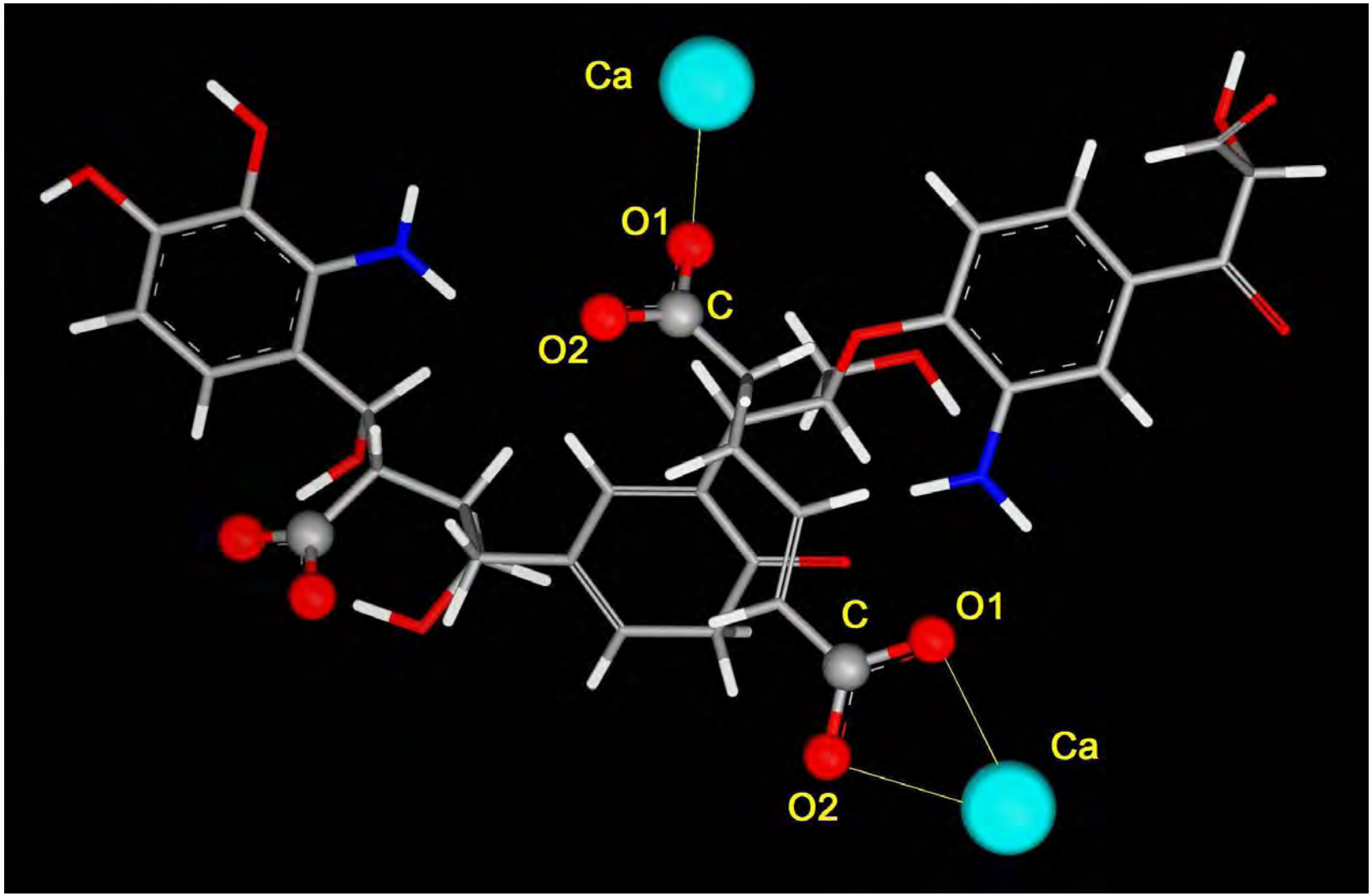

Figure 1.

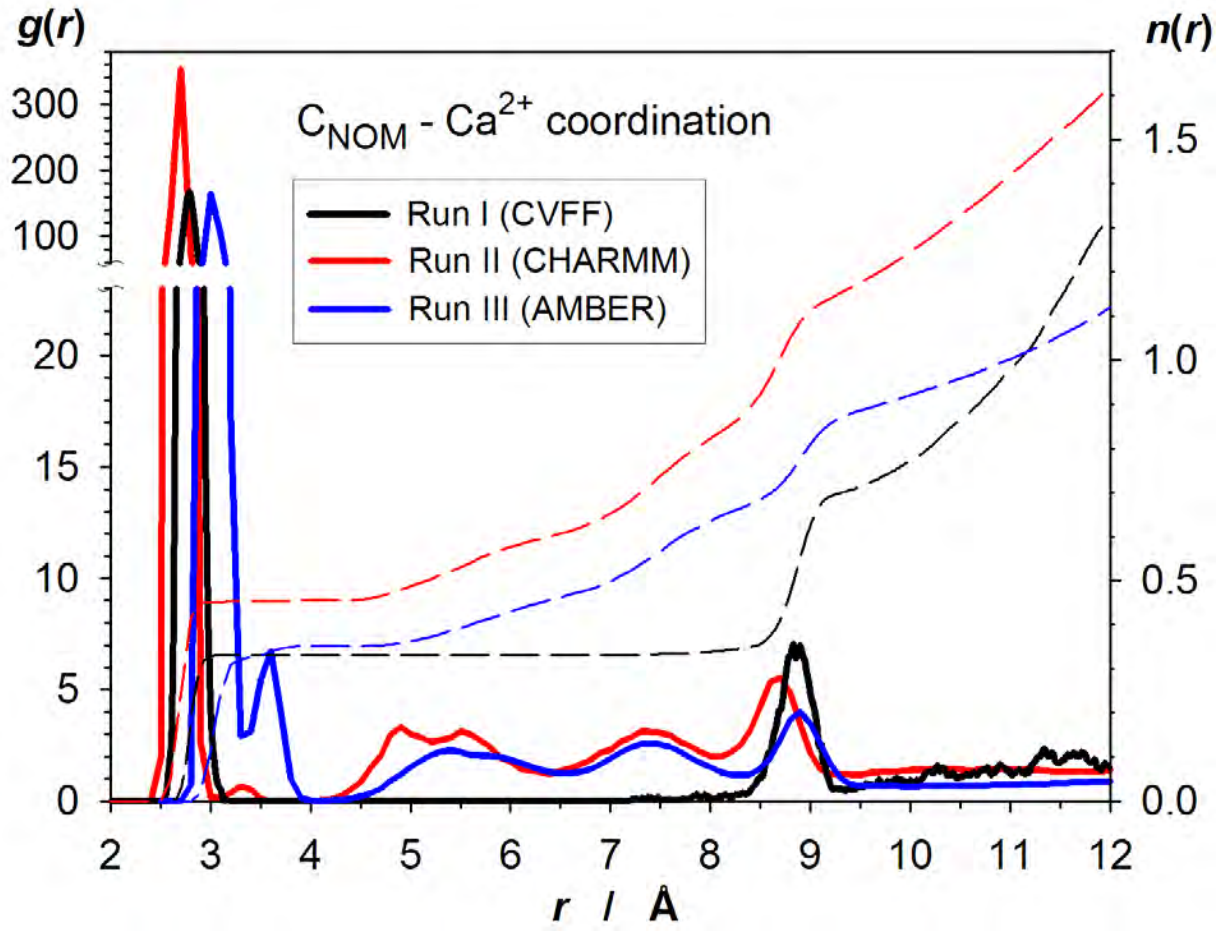
g(r)
n(r)
C_NOM - Ca2+ coordination
Run I (CVFF)
Run II (CHARMM)
Run III (AMBER)
300
200
100
20
15
10
5
0
1.5
1.0
0.5
0.0
2
3
4
5
6
7
8
9
10
11
12
r / Å

Figure 2.

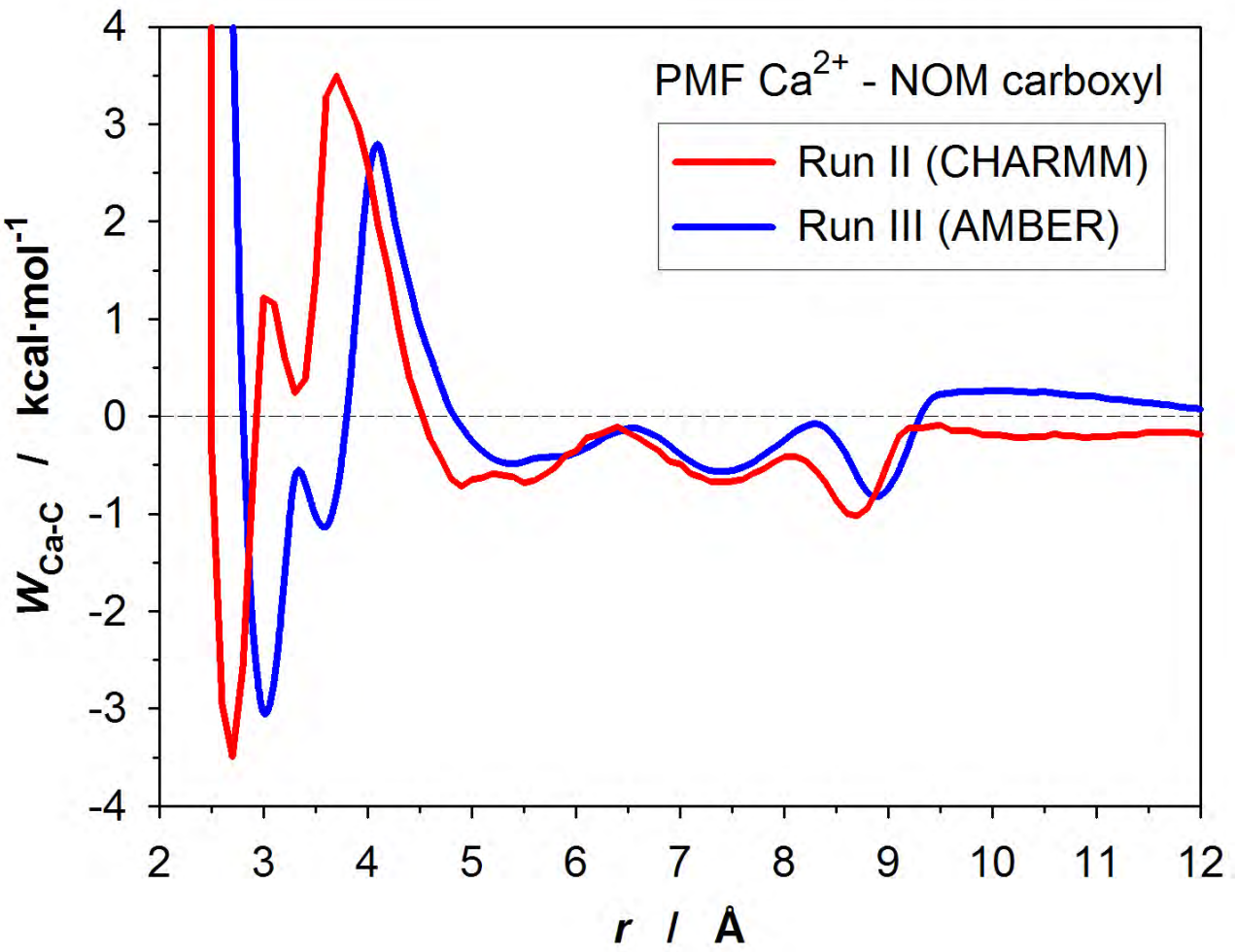
PMF Ca2+ - NOM carboxyl
Run II (CHARMM)
Run III (AMBER)
W Ca-C / kcal·mol-1
r / Å
4
3
2
1
0
-1
-2
-3
-4
2
3
4
5
6
7
8
9
10
11
12

Figure 3.

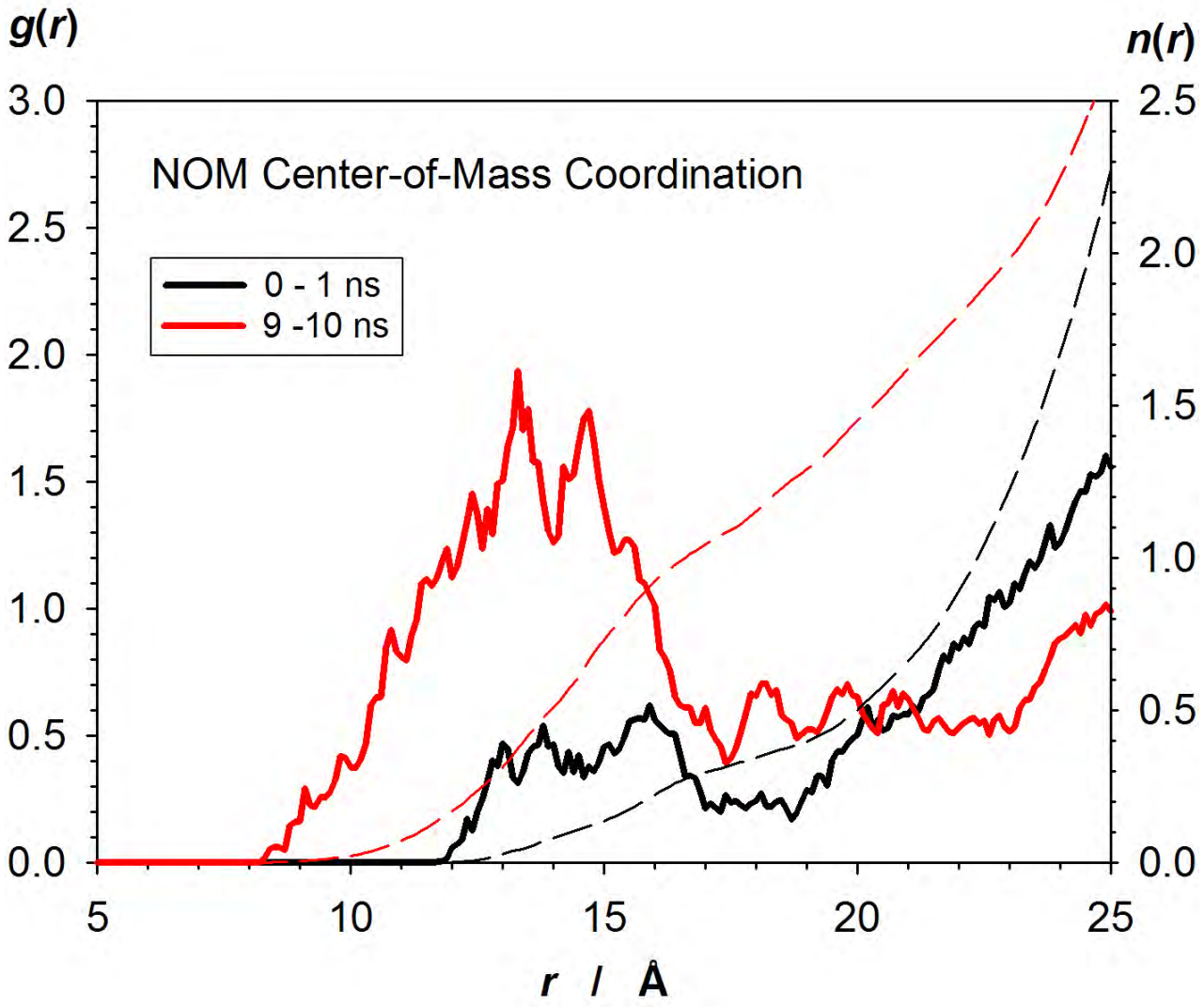
g(r)
n(r)
NOM Center-of-Mass Coordination
0 - 1 ns
9 -10 ns
3.0
2.5
2.0
1.5
1.0
0.5
0.0
2.5
2.0
1.5
1.0
0.5
0.0
5
10
15
20
25
r / Å

Figure 4.

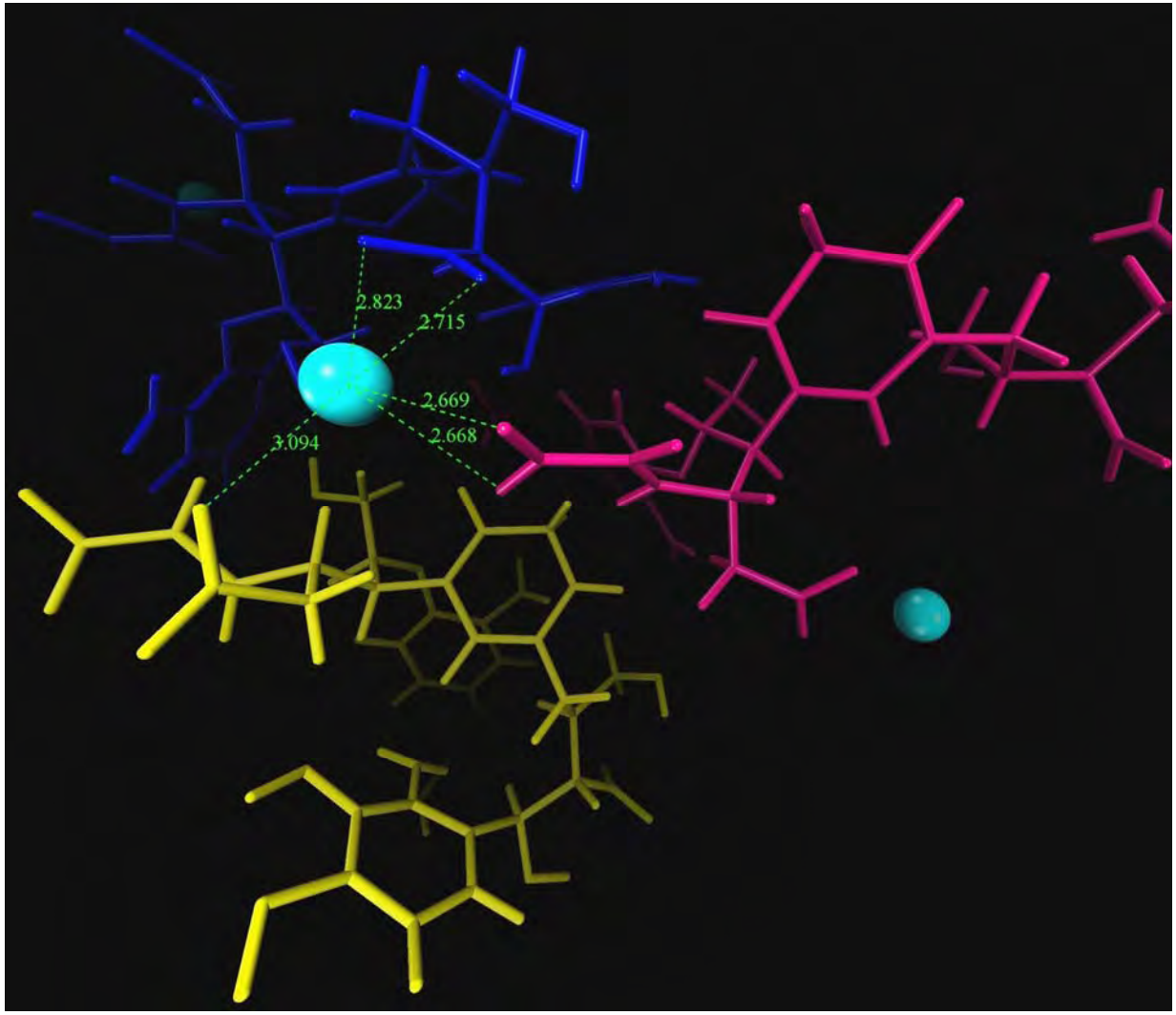

Figure 5.

Research Highlights

- Compositional and structural diversity of NOM impedes its characterization in full atomistic detail
- Nevertheless, the results of computational molecular modeling using a realistic NOM model and several different force fileds are quite robust and consistent
- Ca^{2+} ions associate with 35-50% of the NOM carboxylic groups with a strong preference for the bidentate-coordinated contact ion pairs
- The degree and mechanisms of NOM supramolecular aggregation in the presence of Ca^{2+} are assessed on a semi-quantitative level

Graphical Abstract